Article

Structure of the Fully Modified Left-Handed Cyclohexene Nucleic Acid Sequence GTGTACAC

Koen Robeyns, Piet Herdewijn, and Luc Van Meervelt

J. Am. Chem. Soc., **2008**, 130 (6), 1979-1984 • DOI: 10.1021/ja077313f

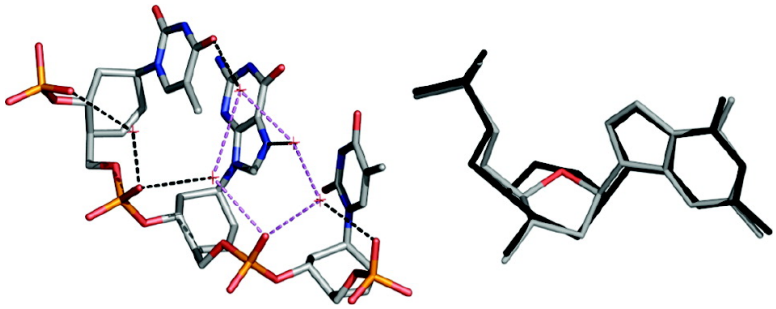

J|A|C|S
ARTICLES
Published on Web 01/17/2008

Structure of the Fully Modified Left-Handed Cyclohexene Nucleic Acid Sequence GTGTACAC

Koen Robeyns, Piet Herdewijn,‡ and Luc Van Meervelt*

Katholieke Universiteit Leuven, Department of Chemistry, Biomolecular Architecture and BioMacS, Celestijnenlaan 200F, B-3001 Leuven, Belgium, and Katholieke Universiteit Leuven, Laboratory of Medicinal Chemistry, Rega Institute for Medical Research and BioMacS, Minderbroedersstraat 10, B-3000 Leuven, Belgium

Received September 21, 2007; E-mail: Luc.VanMeervelt@chem.kuleuven.be

Ⓦ This paper contains enhanced objects available on the Internet at http://pubs.acs.org/journals/jacsat.

Abstract: CeNA oligonucleotides consist of a phosphorylated backbone where the deoxyribose sugars are replaced by cyclohexene moieties. The X-ray structure determination and analysis of a fully modified octamer sequence GTGTACAC, which is the first crystal structure of a carbocyclic-based nucleic acid, is presented. This particular sequence was built with left-handed building blocks and crystallizes as a left-handed double helix. The helix can be characterized as belonging to the (mirrored) A-type family. Crystallographic data were processed up to 1.53 Å, and the octamer sequence crystallizes in the space group *R*32. The sugar puckering is found to adopt the $^{3}H_{2}$ half-chair conformation which mimics the C3′-*endo* conformation of the ribose sugar. The double helices stack on top of each other to form continuous helices, and static disorder is observed due to this end-to-end stacking.

1. Introduction

The structural information on nucleic acids is mostly focused on DNA and RNA, because of their biological function. About 48% of the nucleic acid sequences in the Nucleic Acid Data Bank[1] (NDB) (omitting protein/DNA complexes) consists of unmodified DNA structures, and 27% is unmodified RNA structures determined by either X-ray or NMR, and only about 5% has modifications in the sugar phosphate backbone. Sugar-modified nucleic acids became important at the moment that DNA and RNA were considered as potential therapeutic targets. Striking examples are antigene and antisense applications and more recently, siRNA approaches.

However, synthetic nucleic acids have also been considered in the aptamer field, in investigating life's origin and in diagnostics and nanotechnology.

As long as interactions with DNA and RNA have been considered, research on sugar-modified nucleic acids was aimed at mimicking natural nucleic acids in the A- and B-type conformations (with pre-organization as the basic principle). Until now, no pre-organized, enzymatically stable nucleic acid has yet reached the market.

Due to the many potential applications of sugar-modified nucleic acids, the landscape of structural diversity in the field of double-stranded nucleic acids has broadened considerably (beyond the typical A- and B-type conformations).[2] A second important observation is that it may be advantageous to introduce a certain degree of flexibility in the modified nucleoside to keep the synthesized nucleic acid functional. This may not be the case when the fully modified nucleic acid is used as antagonist (gene blocker), but certainly when some catalytic properties are expected (for example as ribozymes). The alternative, to reach this conformational flexibility and catalytic power, is to use mixmers. Also in the field of the formation of nucleic acid nanostructures, a certain degree of flexibility might be advantageous for building high-order structures.

With this in mind we have synthesized cyclohexene nucleic acids (CeNA). Although the flexibility is less than that of a natural nucleoside (constraints are introduced by the rigid double bond within the six-membered ring), the CeNA cyclohexenyl ring is more flexible than the hexitol sugar ring (schematic representations of the HNA and CeNA monomers are shown in Figure 1). Oligonucleotides containing CeNA residues are capable of forming hybrids with their DNA and RNA analogues, and CeNA/RNA duplexes are more stable than DNA/RNA analogues.[3] CeNAs are currently under investigation for the potential use as the "third nucleic acid" in biotechnological experiments. It has been demonstrated that CeNA can be incorporated in siRNA duplexes with retention of potent

‡ Rega Institute for Medical Research and BioMacS.

(1) Berman, H. M.; Olson, W. K.; Beveridge, D. L.; Westbrook, J.; Gelbin, A.; Demeny, T.; Hsieh, S.-H.; Srinivasan, A. R.; Schneider, B. *Biophys. J.* **1992**, *63*, 751−759.

(2) Nauwelaerts, K.; Lescrinier, E.; Herdewijn, P. *Chem. Eur. J.* **2007**, *13*, 90−98.

(3) (a) Wang, J.; Verbeure, B.; Luyten, I.; Lescrinier, E.; Froeyen, M.; Hendrix, C.; Rosemeyer, H.; Seela, F.; Van Aerschot, A.; Herdewijn, P. *J. Am. Chem. Soc.* **2000**, *122*, 8595−8602. (b) Nauwelaerts, K.; Lescrinier, E.; Sclep, G.; Herdewijn, P. *Nucleic Acids Res.* **2005**, *33*, 2452−2463.

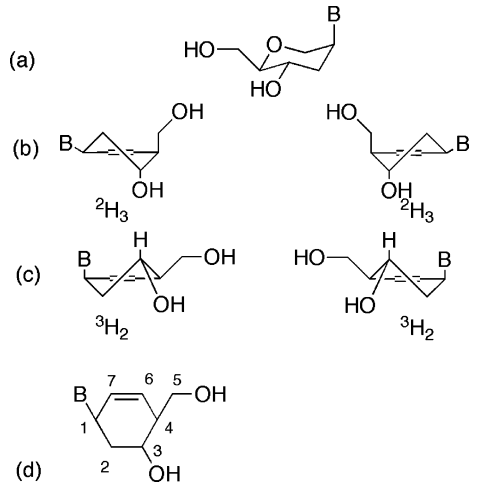

Figure 1. Schematic representation of the HNA (a) and CeNA (b, c) building blocks. For CeNA the two stable left-handed conformations are shown $^2H_3$ (b) and $^3H_2$, (c) half-chair conformations, mimicking the C2′-*endo* or C3′-*endo* conformation of the furanose sugar moiety in natural DNA. For (b) and (c) both the left-handed CeNA residues (left side) and the right-handed CeNA residues (right side) are shown. In (d) the numbering scheme for the left-handed CeNA residues, used in this paper, is shown.

biological activity.[4] In order to obtain more insight in the structure of CeNA and to further broaden the repertoire of non A-, non B-type helices, we have now solved the X-ray structure of the left-handed double-stranded CeNA.

To date, two types of left-handed structures are known: the more irregular Z-DNA known since 1979[5] and the L-RNA sequence r(CUGGGCGG)·r(CCGCCUGG).[6]

L-Oligonucleotides or Spiegelmers are not expected to hybridize with natural nucleic acids. However, they find useful applications in the aptamer field[7] for which L-CeNA might be another candidate. In general nucleic acids with inverted chirality are expected to be more enzymatically stable than natural-like nucleic acids while having the potential of being high-affinity binders.

Enantiomeric nucleic acids might have different hybridization properties when complexed with structurally different oligomers.[8] In the case of self-complementary duplexes, however, the structure of a left-handed helix might act as a model for the structure of the right-handed helix.

To the crystal structures of left-handed nucleic acids we now add the first crystal structure of a fully modified left-handed nucleic acid fragment, where the left-handed helix sense was obtained by using the left-handed CeNA building blocks (Figure 1d).

The geometry of the fully modified left-handed CeNA sequence may give us important information about the potential applicability of CeNA and the influence of the double bond on the hydration and conformation of the duplex.

Table 1. Data Collection Statistics for the Left-Handed CeNA Structure GTGTACAC

λ (Å)	0.8126
space group	*R*32 (hexagonal setting)
cell dimensions (Å)	$a = b = 41.455$ Å, $c = 65.580$ Å
resolution range (Å)	20.00−1.53 (1.58−1.53)[a]
measured reflections	51008
unique reflections	3416
completeness (%)	98.6 (99.7)[a]
R_{symm} (%)	10.8 (37.6)[a]
multiplicity	15.0
mean $I/\sigma(I)$	5.39
χ^2	0.921
reflections with $I > 3\sigma$ (%)	46.2 (29.3)[a]
B-value (Å^2)	17.6
mosaicity (deg)	1.071

[a] Values in parentheses are for the highest resolution shell

2. Experimental Section

2.1. Oligonucleotide Synthesis. The modified cyclohexene nucleotides were synthesized by the Rega Institute. The synthesis results in a racemic mixture of both the left- and right-handed CeNA residues (Figure 1b,c). After enantiomeric purification, the octamer was assembled starting from the left-handed monomers. Both the synthesis of the cyclohexene nucleotides and the assembly into oligonucleotides is described in more detail in Gu et al. (2003).[9] An additional phosphate group was added to the O3′-end to avoid synthesis of the succinate of a cyclohexenyl nucleoside for solid support synthesis.

2.2. Crystallization Conditions. Crystallization conditions of the left-handed CeNA sequence GTGTACAC and preliminary X-ray studies are described in Robeyns et al. (2005).[10]

Additional synchrotron data were collected at the EMBL beamline X11 ($\lambda = 0.8126$ Å) with $\Delta\phi$-increments of 1° to the high-resolution limit of 1.48 Å. The crystals were flash-cooled to 100 K and belong to the rhombohedral space group *R*32 ($a = b = 41.455$ Å, $c = 65.580$ Å; hexagonal setting). Data were integrated and reduced using DENZO and SCALEPACK[11] up to 1.53 Å. Despite the relative high-resolution indexing, the dataset was quite challenging[9] due to the presence of alternating strong and weak reflection layers. Table 1 reports the data collection statistics for the left-handed CeNA structure.

2.3. Structure Determination. The structure of the left-handed CeNA sequence was solved by molecular replacement. Initially the structure was solved in the space group *R*3, using the right-handed HNA structures (NDB code HD0001 and HD0002) as a model.[12] The molecular replacement program Phaser[13] was used to search for two half duplexes, rather than one full duplex, to avoid influence of a different helical curvature between the structure and the MR model. A clear solution stood out in which the two half duplexes could be linked together. The right-handed solution was then converted to the left-handed form, and the molecular replacement procedure was repeated with the complete left-handed model.

It was only during the refinement that it became clear that the two strands were connected by a crystallographic two-fold rotation axis. At this point the data were reprocessed in the correct space group *R*32, with the asymmetric unit consisting of one strand and a solvent content of 43%.

The standard bases were refined using the restraints found in the NDB database;[1] for the cyclohexene sugars, a dictionary of restraints

(4) Nauwelaerts, K.; Fisher, M.; Froeyen, M.; Lescrinier, E.; Van, Aerschot, A.; Xu, D.; Delong, R.; Kang, H. M.; Juliano, R.; Herdewijn, P. *J. Am. Chem. Soc.* **2007**, *129*, 9340−9348.
(5) Wang, A. H. J.; Quigley, G. J.; Kolpak, F. J.; Crawford, J. L.; van Boom, J. H.; Van der Marel, G.; Rich, A. *Nature* **1979**, *282*, 680−686.
(6) Vallazza, M.; Perbandt, M.; Klussmann, S.; Rypniewski, W.; Einspahr, H. M.; Erdmann, V. A.; Betzel, Ch. *Acta Crystallogr.* **2004**, D*60*, 1−7.
(7) Klussmann, S.; Nolte, A.; Bald, R.; Erdmann, V. A.; Fuerste, J. P. *Nat. Biotechnol.* **1996**, *14*, 1112−1115.
(8) Froeyen, M.; Morvan, F.; Vasseur, J.-J.; Nielsen, P.; Van Aerschot, A.; Rosemeyer, H.; Herdewijn, P. *Chem. Biodiversity* **2007**, *4*, 803−817.
(9) Gu, P.; Schepers, G.; Rozenski, J.; Van Aerschot, A.; Herdewijn, P. *Oligonucleotides* **2003**, *13*, 479−489.
(10) Robeyns, K.; Herdewijn, P.; Van Meervelt, L. *Acta Crystallogr.* **2005**, F*61*, 585−586.
(11) Otwinowski, Z.; Minor, W. *Methods Enzymol.* **1997**, *276*, 307−326.
(12) Declercq, R.; Van Aerschot, A.; Read, R. J.; Herdewijn, P.; Van Meervelt, L. *J. Am. Chem. Soc.* **2002**, *124*, 928−933.
(13) McCoy, A. J.; Grosse-Kunstleve, R. W.; Storoni, L. C.; Read, R. J. *Acta Crystallogr.* **2005**, D*61*, 458−464.

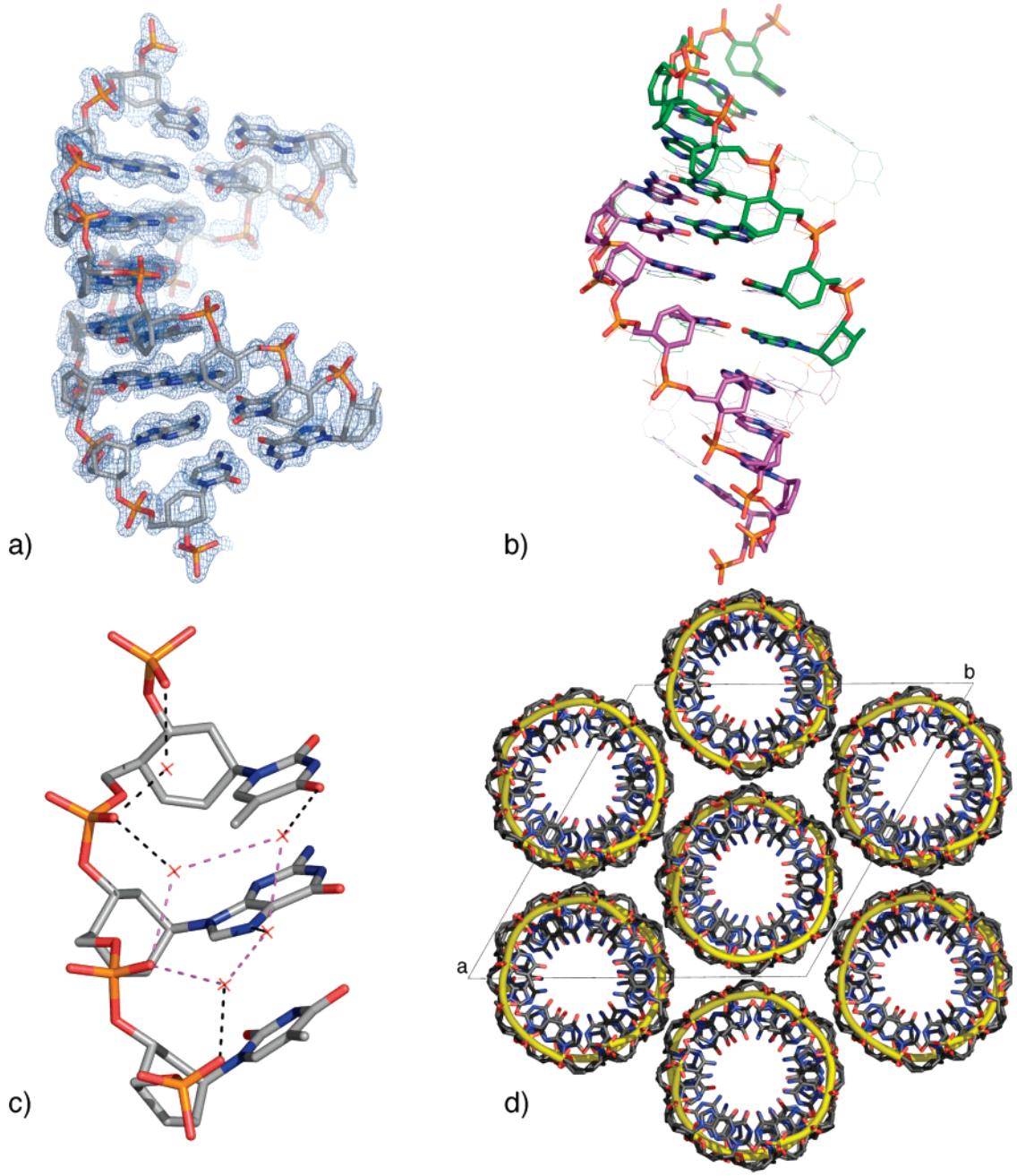

Figure 2. (a) Stick representation of the left-handed CeNA duplex GTGTACAC with electron density maps contoured at the 1.1σ level. (b) Visualization of the static disorder encountered. Part one is colored in green, part two in magenta, both parts are shifted four base pairs to one another. The duplexes are generated by applying the crystallographic two-fold rotation axis, and the symmetry-related strands are represented as lines and colored according to their parts. (c) Part of the CeNA sequence GTGTACAC that shows the bridging water molecules and the pentagonal network. (d) Visualization of the packing observed for the left-handed CeNA helix GTGTACAC. The double helices form continuous columns that are orientated parallel along the *c*-axis (perpendicular to the plane).

Ⓦ Animated representation of the observed disorder in avi format is available.

was built using values found in the CSD.[14] During the refinement, inspection of the density maps and the temperature factors clearly indicated static disorder. The structure was refined in two parts, due to the observed static disorder, using SHELXL-97.[15] The two parts are shifted four base pairs to one another, superposing every adenine base onto a guanine base and every thymine base onto a cytosine base, and the occupancy factors were refined to 49% and 51%. The refinement converged at an *R*-value of 15.8%. Occupancy factors were initially fixed at 50% for the two parts and refined once no significant shifts of atomic coordinates and isotropic temperature factors were observed for all non-solvent atoms. Figure 2a shows the duplex of part one with contoured electron density maps. Despite the disorder the density maps are clear, since the sugar−phosphate backbone as well as the base pairs of both parts occupy common positions (where every G·C base pair is superposed onto an A·T base pair of the other part, and vice versa; electron density maps for the base pairs are provided as Supporting Information).

The atomic coordinates have been submitted in the Protein Data Bank (PDB code 2H0N) and in the Nucleic Acid Data Bank (NDB

(14) Allen, F. H.; Kennard, O. *Chem. Design Aut. News* **1993**, *8*, 31−37.
(15) Sheldrick, G. M.; Schneider, T. R. *Methods Enzymol.* **1997**, *277*, 319−343.

Table 2. Refinement Parameters for the Left-Handed CeNA Structure GTGTACAC

resolution range (Å)	20.00−1.53
total reflections used	3396
numbers of atoms	
CeNA	172
waters (treated as O)	31
data to parameter ratio	2.1
final wR2 (all data) (%)	36.75
R_{free}	n.a.[a]
R-value (R_1; $F_o > 4\sigma(F_o)$) (%)	15.81
rms deviation from restraint target value:	
bond lengths (Å)	0.019
angle distances (Å)	0.025
distances from restraint planes (Å)	0.001
anti-bumping distance restraints (Å)	0.005
mean B-values:	
CeNA (Å^2)	19.0
waters (Å^2)	26.7

[a] n.a.: not available.

code UD0068). The refinement statistics of the left-handed CeNA helix are summarized in Table 2.

3. Results and Discussion

The left-handed CeNA sequence GTGTACAC crystallizes in the space group *R*32. The self-complementary cyclohexene sequence forms an antiparallel left-handed helix in which all bases are engaged in Watson−Crick hydrogen bonding, with hydrogen bonding and C1′···C1′ distances close to the standard values[16] (Figure 2a). The average λ angles (angle between the vectors C1′−C1′ and C1′−N1−N9) for both the purine and pyrimidine bases are quite similar 54.7° and 55.3° respectively. The λ angle for the guanine bases is on average 7° smaller than the angle for the adenine bases, 51.2° and 58.2°, respectively, whereas the λ angles for the two pyrimidine bases are almost the same, 54.7° for the thymine bases and 55.8° for the cytosine bases.

The two static disordered parts (Figure 2b) are connected through a pseudo-two-fold rotation axis, and superposing the two parts using all atoms shows a rms deviation of only 0.38 Å with a maximum deviation of 1.18 Å. Therefore, in further discussion, values and results will refer to part one only.

The CeNA backbone adopts an average conformation for α to ξ respectively +sc, −ap, −sc, −sc, +ac, and +sc. When comparing these torsion angle ranges with the ones observed for naturally occurring DNA, more or less the same values are observed as for A- and B-type DNA, apart from the opposite sign.[15,17]

The cyclohexene rings adopt the $^3H_2$ half-chair conformation (Figure 1b), which was confirmed by analysis of the Cremer and Pople[18] parameters ($\theta = 141°$ and $Q = 0.55$ Å) using the program Platon.[19] The puckering amplitude Q is only slightly higher than the one observed in an ideal cyclohexene chair conformation ($Q = 0.51$ Å). The base is found in the axial position and in the anti conformation, and the nucleoside mimics the C3′-*endo* sugar conformation found in A-type helices (Figure 3). The torsion angle distribution is relatively narrow with small standard deviations, especially for the sugar pucker-related

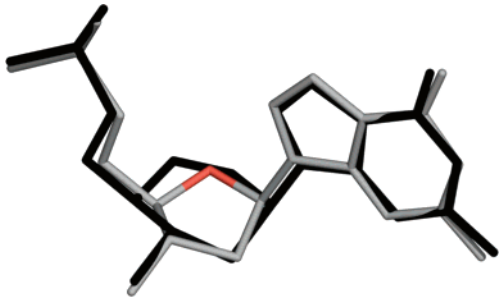

Figure 3. Superposition of a normal DNA guanosine phosphate with the sugar ring in the C3′-*endo* conformation onto its CeNA analogue with the six-membered sugar ring in the $^3H_2$ conformation, converted to its right-handed form.

torsion angles δ and χ.[20] This indicates that the sugar conformation is well defined and that the base is strictly oriented relative to the cyclohexene ring. Moreover, the torsion angle δ adopts an average value of −78°, which is close to the torsion angle value of 81° observed in A-type DNA.[21]

Related to the sugar puckering and backbone torsion angles is the average intrastrand phosphate distance, which is only slightly shorter (5.7 Å) than the value of 5.9 Å observed in A-type DNA.

The temperature factors for the sugars, bases, and phosphates are very comparable with an average value of 19.2 Å^2 for all non-solvent atoms. Unlike the classical trend, in which natural nucleic acid temperature factors increase in the order bases > sugars > phosphates, the B-values of the bases, sugar moieties, and phosphate groups are very similar, that is respective average B-values 20.2 Å^2, 17.2 Å^2, and 22.3 Å^2. This is an indication of rigid sugar−base entities that are firmly packed within the helix structure. This phenomenon was also observed in the HNA structures[11] and suggests that the six-membered sugar rings increase the rigidity of the nucleic acid structure. This rigidity is already illustrated by the small standard deviations on the torsion angles.

Inspection of the helical parameters (Table 3), calculated with the 3DNA package[22,23] reveals an average *x*-displacement of 6.0 Å, indicating that the base pairs are displaced away from the helical axis, which is visible as a central axial hole running through the helix, a feature that is characteristic for A-type DNA.

The base pairs are inclined over 12.7° with respect to the helical axis. The bases show on average nearly no propeller twist which, together with an average buckle of 0.87°, indicates that the base pairs are relatively flat. The planarity of the base pairs might be related to the high slide (−2.7 Å) compared to A-type DNA (−1.53 Å). High slide reduces the ability to propeller twist, which would result in unfavorable electrostatic interactions.[24] The rise is on average 3.3 Å, and a twist of −29.6° is observed. The negative twist clearly shows the left-handed character of the helix, with about 12.2 base pairs in a full turn.

(16) Saenger, W. In *Principles of Nucleic Acid Structure*; Cantor, C. R., Ed.; Springer-Verlag: New York, 1984; pp 116−126.
(17) Torsion angles in left-handed helices show opposite signs with respect to right-handed helices.
(18) Cremer, D.; Pople, J. A. *J. Am. Chem. Soc.* **1975**, *97*, 1354−1358.
(19) Spek, A. L. *J. Appl. Crystallogr.* **2003**, *36*, 7−13.
(20) Since the cyclohexene residues lack the oxygen atom in the ring, the χ torsion angle is defined as C7′−C1′−N1−C2 for pyrimidine bases and C7′−C1′−N9−C4 for purine bases, compared to O4′−C1′−N9−C2 and O4′−C1′−N9−C4 for natural DNA structures, respectively.
(21) Schneider, B.; Neidle, S.; Berman, H. M. *Biopolymers* **1997**, *42*, 113−124.
(22) Because of the different reference frame used in left and right-handed helices, shear, propeller, shift, roll, twist, *x*-displacement, and tip change sign when comparing right-handed helix and left-handed helices. Buckle, stretch, stagger, opening, tilt, slide, rise, inclination, and *y*-displacement can be compared without changing the sign.
(23) Lu, X.-J.; Olson, W. *Nucleic Acids Res.* **2003**, *31*, 5108−5121.
(24) El Hassan, M. A.; Calladine, C. R. *J. Mol. Biol.* **1999**, *259*, 95−103.

Table 3. Helical Parameters for the Left-Handed CeNA Helix and Comparison with the Classical DNA Families and with Its HNA and DNA Analogues

			GTGTACAC structures				
	B-DNA[a]	A-DNA[a]	CeNA	HNA (hex)	HNA (trig)	DNA	L-RNA
x-displacement (Å)	0.05	−4.17	6.0	−6.2	−7.8	−3.1	5.6
inclination (deg)	2.1	14.7	12.7	17.7	9.1	12.6	14.3
rise (Å)	3.32	3.32	3.3	3.3	3.3	3.2	3.3
twist (deg)	36.0	31.1	−29.6	28.9	25.6	32.3	−31.0
slide (Å)	0.23	−1.53	−2.7	−2.2	−2.9	−1.2	−1.8
roll (deg)	0.6	8.0	−6.7	9.9	3.7	6.9	−6.7
propeller twist (deg)	−11.4	−11.8	0.31	1.68	6.11	−12.95	10.2
buckle (deg)[b]	0.5	−0.1	0.00 (0.87)	0.00 (1.31)	0.00 (−1.64)	0.00 (−10.82)	0.7
P···P (Å)	7.0	5.9	5.7	5.5	5.7	6.1	5.9

[a] Helical parameters for A- and B-type DNA are taken from ref 27 and the intrastrand phosphate distances are taken from Saenger (1984).[28] [b] Values in parentheses are for the first four base pair steps. The average value of 0.00 is a result of the crystallographic two-fold symmetry axis.

The left-handed structure GTGTACAC shows base stacking patterns typically observed in A-type DNA. The observed stacking patterns are sequence related in which every purine/pyrimidine step displays only intrastrand interactions, while all pyrimidine/purine steps are characterized by interstrand overlap.

The phosphate groups are highly solvated by water molecules either in a monodentate or bidentate binding mode. Bridging water molecules between phosphate oxygens of two consecutive phosphate groups are commonly observed in A-type helices because of the shorter interstrand P−P distances (average value 5.9 Å) and are also found in the structure of the left-handed CeNA helix (average value 5.7 Å) (Table 3). The hydrogen-bonding network can in some cases form pentagonal rings in A-type DNA, and one such network is also found in the CeNA duplex (Figure 2c).

The symmetry-related helices stack on top of each other by end-to-end stacking. These continuous helices pack in parallel layers orientated along the *c*-axis (Figure 2d). Here the extra phosphate group plays an important role, since it is located in between the stacking helices, making the sugar−phosphate backbone continuous.

This end-to-end stacking directly results in the observed static disorder, which is caused by stacking helices of less than one turn (8 bp) on top of each other, while the helical twist requires more (12) base pairs to complete one helical turn. Similar results are observed when stacking helices are longer than one helical turn.[25]

Superposing the CeNA double helix (converted to the right-handed form) onto its DNA (ADH038) and HNA (HD0001 and HD0002) analogues results in an rms difference of 2.05 Å, 1.56 Å, and 1.74 Å, respectively, highlighting the structural conservatism of these structures.

The solvent accessible surface area (SASA) is considerably larger in the CeNA helix compared to that in the natural analogue (3324 Å^2 vs 3090 Å^2 for the natural analogue) and is almost solely due to an increase of the apolar surface from 1588 Å^2 for the natural analogue to 1892 Å^2 for the CeNA helix.

The double bond in the CeNA residues indeed increases the hydrophobicity of the minor groove. It also eliminates the possibility to form hydrogen bonds between the sugar ring and water molecules. The minor groove width (calculated as the shortest distance between the C7′ atoms on opposite strands) of the CeNA helix (4.12 Å) is also more than two angstroms shorter than the natural DNA analogue (ADH038 6.19 Å). Also the major groove (calculated as the shortest distance between the phosphate atoms on opposite strands) of the DNA analogue is broader (10.40 Å) than the major groove of the CeNA helix (9.86 Å).

The folding of the CeNA into an (left-handed) A-type double helix is very interesting for applications in the antisense field. A-type helices do not normally stack in infinite helices, a characteristic which is normally ascribed to B- and Z-type DNA. Compared with B-type duplexes, A-type duplexes expose their hydrophobic regions of the sugar−phosphate backbone more in the minor groove. The folding of the CeNA sequence into A-type DNA is believed to arise from the larger hydrophobic regions in this sugar−phosphate backbone. The reduction of donor/acceptor sites in the sugar−phosphate backbone disrupts hydrogen bonds in the minor groove, especially in ordered water networks (such as the "spine of hydration") commonly found in B-type DNA. The double helix copes for the loss of donor/acceptor sites by adapting to the more economical hydration of A-type DNA. Furthermore the $^3H_2$ half-chair conformation, which mimics the C3′-*endo* conformation commonly found in A-type helices, is shown to be the preferred conformation for all four nucleobase monomers.[3b]

4. Conclusions

Recently, modified nucleic acids have become an important synthetic target. However, only limited structural information is known about these modified nucleic acids. We now present the molecular and crystal structure of the first fully modified left-handed structure.

The presently available X-ray structures of modified nucleic acids have been generated using oxygen-containing rings such as furanose, pyranose, and hexitol rings in their backbone. This CeNA duplex is the first example of an X-ray structure of a carbocyclic-based nucleic acid, with only carbon atoms in the sugar ring.

The cyclohexene nucleic acid sequence GTGTACAC, built from left-handed CeNA building blocks, crystallizes in the rhombohedral space group *R*32. Data were collected up to 1.48 Å and processed with a cutoff at 1.53 Å. As expected, the helix was found to be an antiparallel left-handed duplex. A crystallographic two-fold axis runs through the duplex, connecting the two strands and resulting in an asymmetric unit of a half helix. The base pairs consist of normal Watson−Crick base pairs with hydrogen bonds with lengths that are similar to the standard values. The backbone torsion angles occur in relatively well-defined regions, especially the sugar-related torsion angles δ

(25) Shah, S. A.; Brunger, A. T. *J. Mol. Biol.* **1999**, *285*, 1577−1587.

and χ. The helix was classified as belonging to the A-type family, with the characteristic axial hole, resulting in a high *x*-displacement. The CeNA sugar moiety adopts the $^3H_2$ half-chair conformation, which mimics the C3′-*endo* sugar conformation found in A-type helices.

Both interstrand and intrastrand base stacking is found, which turns out to be sequence related. Because of the missing oxygen atom in the sugar ring, the minor groove is quite hydrophobic. On the contrary the phosphate groups are found to be part of numerous hydrogen bonds with localized water molecules. The static disorder that is observed is a direct result of the end-to-end stacking of neighboring helices in which the additional phosphate group acts as a bridge between consecutive helices.

Recently, the crystal structure of a β-homo-DNA duplex, [dd-$(CGAATTCG)_2$], was solved to a resolution of 2.7 Å.[26] In β-homo-DNA the sugar moiety consists of a six-membered sugar ring as well; here, the extra carbon atom is introduced in the front side of the ring (in comparison with CeNA, where two extra carbon atoms are introduced at the backside of the ring, replacing the ring oxygen atom), which results in the formation of a different helix structure.

The double-stranded β-homo-DNA structure resembles natural DNA in its base pairing behavior since it forms an antiparallel duplex with Watson−Crick base pairing. Unlike CeNA oligonucleotides β-homo-DNA cannot form duplexes with natural DNA and RNA. The average twist is only about 14° (or 10.6° omitting the flipped out bases), which makes it quite linear, and the individual steps exhibit highly irregular twists. Also the rise varies considerably, with an average rise of 3.8 Å.

The interstrand phosphate distances are similar to the distances observed in A-type DNA and resemble the interstrand distances in the CeNA structure. The base stacking in the β-homo-DNA structure differs considerably from the base stacking observed in the CeNA octamer. There is a virtual absence of intrastrand stacking, which makes the structure of the β-homo-DNA different from A- and B-type DNA.

Because of the irregular twist and the rather ladderlike structure and the inability to bind with DNA and RNA, β-homo-DNA has no applications in the antisense or RNAi field. The structure determination of the β-homo-DNA duplex was also part of a systematic investigation of the question "why pentose and not hexose?" rather than exploring modified nucleic acids for therapeutic applications. This CeNA structure contributes to a further understanding and mapping of the structural diversity of double-stranded nucleic acids, beyond the classical Watson−Crick model. If we position the left-handed CeNA structure in the landscape of "twist and slide"[2] we see that the mirror image form would be situated in the favorable region which has been demonstrated experimentally, as is the RNA Spiegelmer,[6] while the β-homo-DNA duplex lies close to the edge of this region with stacking distances that tend to be too high.

The present structure contributes to a better understanding of the landscape of potential double-stranded nucleic acids, and we continue our efforts to further explore the synthesis and structure of sugar-modified nucleic acids.

Acknowledgment. We thank the staff of the EMBL Hamburg outstation for their help with the synchrotron experiments and A. Van Aerschot for the synthesis of the oligonucleotide. We thank the K.U. Leuven and FWO for financial support. BioMacS, the K.U. Leuven Interfacultary Centre for Biomacromolecular Structure, is supported by the Impulse Project of the K.U. Leuven.

Supporting Information Available: $2|F_o| - |F_c|$ electron density maps for the individual superposed base pairs of part one and two, as they are present in the crystal structure. This material is available free of charge via the Internet at http://pubs.acs.org.

JA077313F

(26) Egli, M.; Pallan, P. S.; Pattanayek, R.; Wilds, C.; Lubini, P.; Minasov, G.; Dobler, M.; Leumann, C. J.; Eschenmoser, A. *J. Am. Chem. Soc.* **2006**, *128*, 10847−10856.
(27) Olson, W. K.; Bansal, M.; Burley, S. K.; Dickerson, R. E.; Gerstein, M.; Harvey, S. C.; Heinemann, U.; Lu, X. J.; Neidle, S.; Shakked, Z.; Sklenar, H.; Suzuki, M.; Tung, C. S.; Westhof, E.; Wolberger, C.; Berman, H. M. *J. Mol. Biol.* **2001**, *313*, 229−237.
(28) Saenger, W. In *Principles of Nucleic Acid Structure*; Cantor, C. R., Ed.; Springer-Verlag: New York, 1984; pp 261−267.